STARBURST BLOWN SUPERBUBBLES: GAS METALICITY AND X–RAY EMISSION

S. Silich[1,2] and G. Tenorio-Tagle[2]

[1]*Main Astronomical Observatory, NAS of Ukraine*
27 Akademika Zabolotnoho, 03680 Kyiv, Ukraine
e-mail: silich@mao.kiev.ua; silich@inaoep.mx

[2]*Instituto Nacional de Astrofisica Optica y Electronica, AP 51, 72000 Puebla, Mexico*
e-mail: gtt@inaoep.mx

The X-ray emission from star forming regions in different types of galaxies is discussed. Special attention is paid to cases with an obvious discrepancy between model predictions and observed X-ray luminosities. A new solution of this problem, based on time dependent calculations of the X-ray emitting gas metalicity, is here given. Our results show that supernovae metal ejection leads to a high overabundance of the hot bubble interior, that allows for up to an order of magnitude higher X-ray luminosities compared with standard predictions.

INTRODUCTION

Interstellar bubbles, holes, and expanding shells are common astrophysical phenomenon. They are observed around Wolf-Rayed (WR) and O stars, luminous blue variables, and planetary nebulae. On the larger scale, bubbles are produced by the collective action of stellar winds and supernova explosions within OB associations. This coherent massive stars activity reaches an extreme limit in the giant star-forming regions of young starburst galaxies, with thousands and billions of stars concentrated within local (several hundred parsecs) central regions.

These objects can be observed in a variety of energy bands from radio to visible, but the most direct probe for the bubble basic properties is provided by their X-ray emission. Indeed, while the optical lines arise in the dense partly ionized shell segments, which occupy only a small volume, the X-ray emission comes from the hot bubble interior, which contains all starburst (SB) produced energy, mass and metals, and fills most of the SB disturbed volume. X-ray observations, therefore, provide many straightforward restrictions on the star forming region parameters and highly constrain the possible theoretical scenarios.

Here we briefly review most recent X-ray observational results related to multisupernovae activity in different types of the galaxies. We stress the existing discrepancies between the model standard predictions and observed X-ray luminosities. We then propose a new approach to reconcile the observations with the model predictions, and demonstrate that the standard X-ray bubble model may underestimate the X-ray luminosity by almost an order of magnitude.

THE STANDARD BUBBLE MODEL

The observed shells can be tentatively classified into three distinct categories. The smallest ones (type S) are produced by a wind or explosion of a single individual star. Large bubbles (type L) result from the correlated action of a few to several tens of star members of a typical OB-association, and huge ones (type H) result from violent, space correlated star forming activity in SB galaxies.

The general understanding of the observed properties of bubbles is based on the standard bubble model (see Figure 1), which consists of four zones: a) freely expanding wind; b) hot shocked wind; c) dense shell; and d) external ISM [20]. For a moderate energy deposition, the shell cools during the early evolution, and the X-ray emission comes mainly from the hot shocked wind contaminated with interstellar gas evaporated from the cold outer shell as well as from small interstellar clouds disrupted by hydrodynamic instabilities and thermal evaporation.

The X-ray emissivity in the ROSAT 0.1–2.4 KeV energy band is little dependent on temperature within the wide energy range $\sim 10^6 - 10^8$K, and as a first approximation it may be taken to be constant

$$\Lambda_x \approx 3\,\xi \times 10^{-23}\,\mathrm{erg\ s^{-1}}, \tag{1}$$

where ξ is the gas metalicity. This fact has been used by Chu & Mac Low [3], who proposed a rather simple

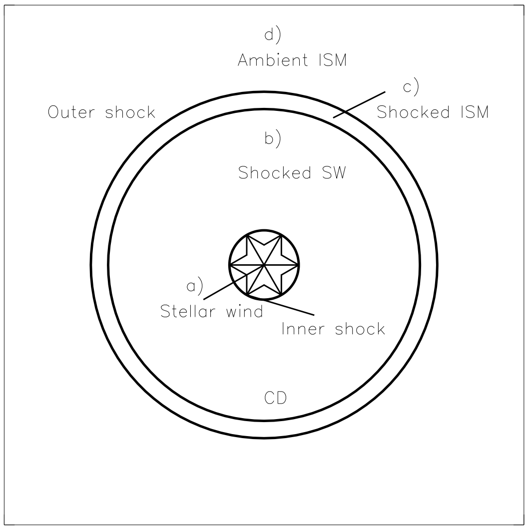

Figure 1: The structure of interstellar bubbles

analytical model for a spherical bubble evolving in a constant density medium. They found (using Weaver *et al.* [20] density and temperature profiles) that the X-ray luminosity of the shocked wind region can be expressed as:

$$L_x = 10^{36} \xi I(\tau) L_{38}^{33/35} n_{ISM}^{17/35} t_7^{19/35} \, \mathrm{erg\, s^{-1}}, \tag{2}$$

where L_{38} is the wind mechanical luminosity in 10^{38} erg s^{-1} units, and t_7 is the elapsed time in 10^7 yr units, n_{ISM} is the ambient gas number density, and ξ is the ISM gas metalicity in Solar units. $I(\tau)$ is a dimensionless integral

$$I(\tau) = \frac{125}{33} - 5\tau^{1/2} + \frac{5}{3}\tau^3 - \frac{5}{11}\tau^{11/2}, \tag{3}$$

where τ is the ratio of the X-ray cutoff temperature ($T_{cut} \sim 10^5$K) to the bubble central temperature.

Note that in this model most of the soft X-ray radiation comes from the rather thin outer bubble layers. For mass loading bubbles this leads to a more picked in time X-ray luminosity, but does not change the maximum value significantly (particularly if one assumes that the additional mass from the cloud destruction process is homogeneously distributed throughout the bubble volume [14]).

LMC BUBBLES AND THE X–RAY DISCREPANCY

Due to its proximity and almost face-on position the Large Magellanic Cloud (LMC) provides an excellent possibility to study individual massive star clusters and their connection to the surrounding medium. The photometric, spectral, X-ray and neutral hydrogen observations constrain the main input model parameters that one needs to compare the model predictions with the observed values.

Chu & Mac Low [3] have examined the *Einstein Observatory* catalog for 75 LMC OB associations and revealed diffuse X-ray emission around 15 of them. The regions with X-ray excess correlate well with the H_α emission, and can be associated to hot L-type bubbles. The bubble X-ray luminosities range from $7{\times}10^{34}$ to $7{\times}10^{36}$ erg s^{-1}. The comparison of the observed values with the model predictions revealed an intriguing result: **most of the X-ray bright bubbles have an X-ray luminosity more than an order of magnitude larger than the expected value**.

This study was later confirmed with ROSAT data, and several X-ray dim bubbles (DEM 31, DEM 105, DEM 106, and DEM 137) have also been analysed. However, in these cases the calculated X-ray emission is comparable with the ROSAT observational limit, and deeper exposure, or more sensitive observations are needed to determine their real X-ray luminosities. In fact the only confirmed exception to date in the LMC is H II complex N11 [6].

Note that X-ray bright and X-ray dim objects also demonstrate different hydrodynamical properties. The X-ray luminous bubbles show an obvious "growth rate discrepancy", *i.e.*, their expansion velocities are found to exceed the model predicted value for a given bubble radius [8].

X–RAY BUBBLES IN NEARBY STAR–FORMING GALAXIES

Large neutral hydrogen cavities and expanding shells have been found in many (if not in all) of the nearby galaxies with a moderate star formation activity (see for review [2]). These cavities are believed to have been blown in the ISM by strong stellar winds and subsequent correlated supernova explosions within massive OB associations containing of few to several hundreds of stars with $M \geq 8\,M_{\odot}$. Within the framework of the general theory these cavities are expected to by filled with hot, supernovae heated gas, and have to be traced as patches of the powerful diffuse X-ray emission. Several attempts recently have been undertaken to confirm this theoretical predictions by direct X-ray observations. However, the observational evidence still remains very scarce.

Walter *et al.* [19] provided a multiwavelength study of a giant neutral hydrogen shell in the north-east quadrant of the nearby dwarf galaxy IC 2574, which is a member of the M81 cluster of galaxies. This shell with $1000{\times}500$ pc size and $\sim$25 km s^{-1} expansion velocity was observed with ROSAT PSPC camera. The observations recovered a diffuse X-ray emission with a luminosity $L_x \approx 1.6{\times}10^{38}$ erg s^{-1} in the 0.1–2.4 KeV energy band. As it was estimated in [19] this luminosity is also about an order of magnitude higher than that predicted by the model [3].

The opposite problem is also well represented by another member of the M81 group. The dwarf irregular galaxy HoII has been well studied in the 21 cm wavelength band by Puche *et al.* [12] and exhibits a violent ISM, which contains a total of 51 neutral hydrogen holes of different sizes and expansion velocities. This galaxy is one of the most luminous dwarf irregulars. However, Zezas *et al.* [21] have demonstrated that the X-ray emission comes only from a single point source embedded into a large H II region. The high X-ray luminosity ($L_x \approx 3{\times}10^{40}$ erg s^{-1}) and the short (days) and long (years) time variability favor a compact supernova remnant or a massive X-ray binary origin of this emission. The mass of the accreting object, however, was estimated to be $\sim$ 200 $M_{\odot}$, well in excess of the mass limit for a stellar black hole candidate. However, the most unexpected result in the framework of our consideration is the lack of diffuse X-ray emission from the numerous HI hole population. To add to the confusion Rhode *et al.* [13] have proclaimed that at least in several of the Holmberg II holes the observed stellar cluster brightness is strongly inconsistent with that predicted by the coherent supernovae model value.

X–RAY EMISSION FROM STARBURST GALAXIES

Coherent stellar winds and supernovae explosions gain their peak activity in starburst galaxies, where the present rate of star formation may be supported only for a small fraction of the Hubble time and is concentrated in a small fraction of the space volume. Usually young stars are concentrated in luminous H_{α} knots as in VII Zw403 galaxy. The energy output rate in the starburst region exceeds that of the rest of the galaxy $L_{SB} \gg L_{gal}$. The common believe is that in many cases this activity leads to a powerful gas outflow from the SB region, which sometimes is even able to remove an essential fraction of the ISM and supernovae produced metals off a galaxy [5]. However, this conclusion is still a matter of comprehensive analysis and debates. Recent numerical studies [15, 4] have shown that in the presence of the dark matter and extended gaseous halos the ISM ejection efficiency is much below than what it was expected by previous studies.

Now, let us make a quick survey of nearby X-ray emitting galaxies with violent star forming activity.

NGC 5253 is one of the nearest (4.1 Mpc) and the youngest up to date known starburst. WR stars identified in two of the five central massive star clusters constrain the age to 3–5 Myr only. An extended soft X-ray emission with $L_x \approx 6.5{\times}10^{38}$ erg s^{-1} from the central part of the galaxy has been revealed by Martin & Kennicutt [7]. They also found that the simple superbubble model underpredicts the NGC 5253 X-ray luminosity by a factor of 16. Strickland & Stevens [17], however, revealed instead of a single huge bubble a system of at least five sources of X-ray emission connected with the young massive star clusters. The X-ray luminosities of the individual components range between $(2\text{–}7){\times}10^{37}$ erg s^{-1}, which is in a better agreement with the model predictions.

VII Zw403 is the nearest blue compact dwarf (BCD) galaxy. This is an isolated system with a total mass $2{\times}10^{8}\,M_{\odot}$, a neutral hydrogen mass of $7{\times}10^{7}\,M_{\odot}$, and a low interstellar gas metalicity $Z = 0.06\,Z_{\odot}$, also considered as a member of the M81 group. Recent HST observations, however, moved it 1.5 kpc farther away, to a 4.5 Mpc distance. Papaderos *et al.* [9] revealed an extended round kpc-scale region of the diffuse X-ray emission with the total X-ray luminosity $L_x \approx 2.3{\times}10^{38}$ erg s^{-1}. Our estimations show the same, as in LMC, IC 2574 and NGC 5253, a more than an order of magnitude difference between the observed X-ray luminosity and the standard model prediction.

NGC 1569. The ASCA 0.5–6 KeV broad-band observations showed an extended X-ray emission. The total X-ray luminosity was estimated to be $L_x \approx 3.1{\times}10^{38}$ erg s^{-1} and may be best fitted with two spectral components. The soft component is best described by a hot plasma model with temperature T=(0.6–0.8) KeV that provides around 60% of the total X-ray emission. It is clearly extended and associated with the system of H_{α} filaments.

About 40% of this emission comes from the unresolved central region, whereas the rest comes from the extended diffuse component.

NGC 253 is one of the three nearest galaxies with prominent superwind features. It presents an extended X-ray region 9 kpc along the galaxy minor axis, and also shows a large number of X-ray point sources both in the mid-plane of the galaxy and its vicinity. The ASCA [11] and BeppoSAX [10] observations revealed soft (0.5–2.0) KeV and hard (2.0–10.0) KeV emission with luminosities $L_x \approx 7.7\times10^{39}$ erg s^{-1} and $L_x \approx 1.6\times10^{40}$ erg s^{-1}, respectively. These observations allowed to estimate the hot inner bubble gas metalicity. The absolute abundances were best estimated to be $Z_{Fe} = 0.25\,Z_\odot$ for iron, and $Z_\alpha = 1.7\,Z_\odot$ for α-elements, however, still remain highly model-dependent. The relative abundances are more definite and confirm an obvious overabundance of the α-elements.

METALICITY OF SUPERBUBBLES

Careful analysis of the X-ray data has led thus to the conclusion that in many cases the observed X-ray luminosities are in clear disagreement with the standard model predictions. Here we relax the standard model assumption which associates the inner bubble metalicity with those of the surrounding ISM. This assumption is being recognized as an idealization due to the contact discontinuity that inhibits mixing of SN ejected metals with the surrounding ISM [18]. The total amount of gas ejected by supernovae (SNe) includes an important fraction of newly synthesized metals and these are well mixed with the thermalized ejected matter and the gas that evaporates from the cold radiative shell segments. Consequently, **the metals ejected by sequential SNe are to be found in the hot bubble interior, causing drastic changes to its metalicity. The later is important because the main contribution to the soft X-ray band comes from the emission lines of oxygen and others α-elements**.

Our initial model includes: a Salpeter initial mass function for a star cluster mass distribution and reasonable approximations for massive stars, main sequence life times, and oxygen yields.

The galaxy model incorporates stars, a dark matter component and a low abundance ($Z = 0.1\,Z_\odot$) ISM, which allows for two isothermal components. One is related to a central dense molecular disk with a mass of 5×10^7 $M_\odot$ and the second represents the low density, extended neutral halo. In all cases the total mass of the host galaxy amounts to be $10^{10}\,M_\odot$, while the gas mass amounts to only $10^9\,M_\odot$. To follow the bubble evolution we used our 3D numerical code, based on the thin layer approximation [1, 15].

THE RESULTS OF THE CALCULATIONS

The calculations [16] follow the bubble time evolution and the change in metalicity of the hot bubble interior due to the SB ejected metals, mixing with the shell evaporated matter. Figure 2 shows the evolution of the metalicity of the superbubble interior as a function of time. It reaches $Z_O \sim 2\,Z_\odot$ after 6 Myr of evolution that is 20 times of the assumed ISM metalicity ($Z_{ISM} = 0.1\,Z_\odot$), falling below solar metalicity just after 10 Myr to slowly approach $0.1\,Z_\odot$ at the end of the calculation. This consequently leads to an enhance X-ray luminosity.

Figure 3 shows the time evolution of L_X for a bubble blown by $10^6\,M_\odot$ starburst. The dotted line represents the standard model with a fixed gas metalicity $Z = 0.1\,Z_\odot$. It reaches first rather a high value of about 10^{39} erg s^{-1}. During this stage, however, the main contribution to a total X-ray emission comes from the adiabatic shell rather than from the hot bubble interior. The shell contribution to the total X-ray emission is most important immediately after blow-out of the remnant from the central gas component into the extended halo of the host galaxy, when the shock reaches speeds of several hundreds of km s^{-1} that lead to the high post-shock temperature of $T \sim 1.4\times10^7\, v_{shock}^2$. The shell contribution becomes rapidly less important as the shock slows down and the shell cools below the X-ray cut-off temperature ($\sim 5\times10^5$) and condenses into a narrow and dense outer boundary of the superbubble. Later on, the main contribution to the bubble X-ray emission comes from the hot bubble interior, marking a dramatic difference between the standard model (dotted line) and of calculations with a time dependent gas metalicity (solid line). The X-ray luminosity reaches approximately an order of magnitude larger values after 10Myrs of evolution caused mainly by an enhanced inner gas metalicity. In this case the luminosity of the superbubble interior is found to remain within the range of $10^{38} - 5\times10^{39}$ erg s^{-1} throughout the evolution.

CONCLUSION

The calculations presented here show large differences in the hot interior gas metalicity with respect to the outer ISM value. The effect of new metals injected into the superbubble interior is most noticeable during the first 10 Myr. If oxygen is used as a tracer, the hot gas abundance reaches values well above solar immediately after the start of the SN phase. It reaches the maximum value after 3 to 5 Myr from the beginning of SN explosions. Later, mixing with the evaporated mass slowly reduces the impact of SNe metal ejection.

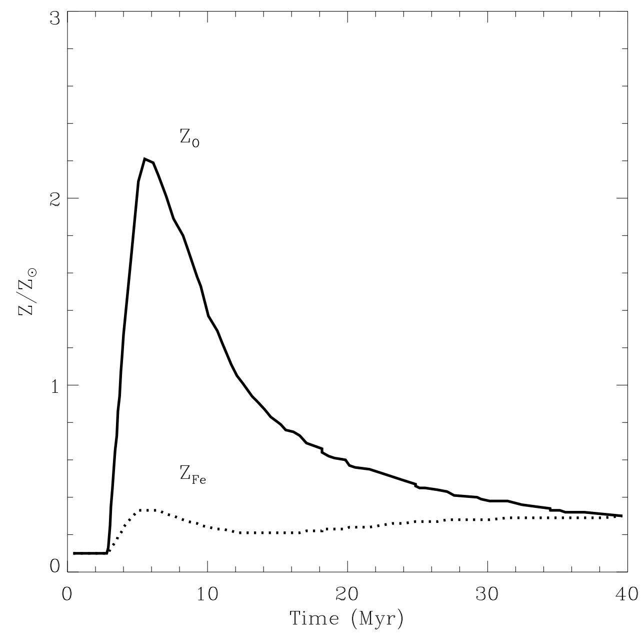

Figure 2: The hot bubble interior oxygen metalicity as function of time

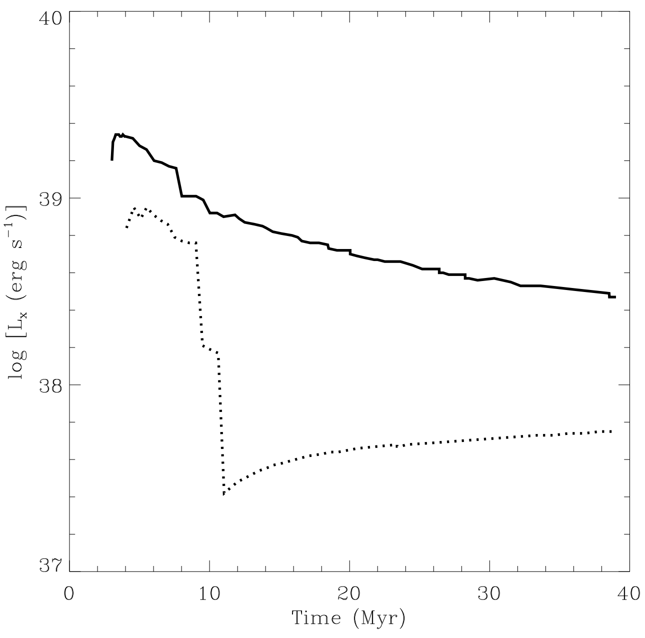

Figure 3: The calculated bubble X-ray luminosity (solid line) as it is compared with the standard bubble model (dashed line)

The most important conclusion is that the enhanced metalicity of superbubble interiors can strongly influence their X-ray luminosity, bringing theory and observations into a better agreement.

Acknowledgments. The authors acknowledge support from IoA Cambridge, where all calculations have been performed. They also highly appreciate fruitful discussions with their collaborators Elena and Roberto Terlevich and Hagai Netzer.

REFERENCES

[1] *Bisnovatyi-Kogan G., Silich S.* Shock-wave propagation in the nonuniform interstellar medium // Rev. Mod. Phys.–1995.–**67**.–P. 661–712.

[2] *Brinks E.* The cool phase of the Interstellar Medium: Atomic gas // The interstellar Medium in Galaxies / Eds H. A. Thronson and J. M. Shull.–Netherlands: Kluwer Acad. Publ., 1990.–P. 39–65.

[3] *Chu Y.-H., Mac Low M.-M.* X-rays from Superbubbles in the Large Magellanic Cloud // Astrophys. J.–1990.–**365**.–P. 510–521.

[4] *D'Ercole A., Brighenti F.* Galactic Winds and Circulation of the ISM in Dwarf Galaxies // Mon. Notic. Roy. Astron. Soc.–1999.–**309**.–P. 941–954.

[5] *De Young D., Heckman T.* The effect of central starbursts on the interstellar medium of dwarf galaxies // Astrophys. J.–1994.–**431**.–P. 598–603.

[6] *Mac Low M.-M., Chang T. H., Chu Y.-H., et al.* X-rays from Superbubbles in the Large Magellanic Cloud V. The H II Complex N11 // Astrophys. J.–1998.–**493**.–P. 260–273.

[7] *Martin C. L., Kennicutt Jr.* Soft X-ray emission from NGC 5253 and the ionized interstellar medium // Astrophys. J.–1995.–**447**.–P. 171–183.

[8] *Oey M. S.* The dynamics of Superbubbles in the Large Magellanic Cloud // Astrophys. J.–1996.–**467**.–P. 666–675.

[9] *Papaderos P., Fricke K. J., Thuan T. X., Loose H.-H.* Hot gas outflow in the blue compact dwarf galaxy VII Zw 403 // Astrophys. J.–1994.–**291**.–P. L13–l16.

[10] *Persic M., Mariani S., Cappi M., et al.* BeppoSAX detection of the Fe K line in the nearby starburst galaxy NGC 253 // Astron. and Astrophys.–1998.–**339**.–P. L33–L36.

[11] *Ptak A., Serlemitsos P., Yaqoob T., Mushotzky R.* The complex X-ray spectra of M82 and NGC 253 // Astron. J.–1997.–**113**.–P. 128–134.

[12] *Puche D., Westpfahl D., Brinks E., Roy J.-R.* // Astron. J.–1992.–**103**.–P. 1841–1858.

[13] *Rhod K. L., Salzer J. J., Westpfahl D. J., Radice L. A.* A test of the standard hypothesis for the origion of the HI holes in Holmberg II // Astron. J.–1999.–**118**.–P. 323–336.

[14] *Silich S., Franco J., Palous J., Tenorio-Tagle G.* Three-dimensional calculations of the evolution of Superbubbles in a cloudy medium // Astrophys. J.–1996.–**468**.–P. 722–738.

[15] *Silich S., Tenorio-Tagle G.* On the fate of processed matter in dwarf galaxies // Mon. Notic. Roy. Astron. Soc.–1998.–**299**.–P. 249–266.

[16] *Silich S., Tenorio-Tagle G., Terlevich R., et al.* Evolution of the X-ray luminosity and metallicity of starburst blown superbubbles // Mon. Notic. Roy. Astron. Soc.–2001.–**324**.–P. 191.

[17] *Strickland D. K., Stevens I. R.* Multiple superbubbles in the starburst nucleus of NGC 5253? Implications for mass loss from dwarf galaxies // Mon. Notic. Roy. Astron. Soc.–1999.–**306**.–P. 43–63.

[18] *Tenorio-Tagle G.* Interstellar Matter Hydrodynamics and the Dispersal and Mixing of Heavy Elements // Astron. J.–1996.–**111**.–P. 1641–1650.

[19] *Walter F, Kerp J., Duric N., et al.* X-ray emission from an expanding supergiant shell in IC 2574 // Astrophys. J. Lett.–1998.–**502**.–P. L143–L147.

[20] *Weaver R., McCray R., Castor J., et al.* // Astrophys. J.–1977.–**218**.–P. 377.

[21] *Zezas A. L., Georgantopoulos I., Ward M. J.* ROSAT observations of the dwarf starforming galaxy Holmberg II (UGC 4305) // Mon. Notic. Roy. Astron. Soc.–1999.–**308**.–P. 302–308.